

Ultrafast spin-polarized electrical currents injected in a strained zinc blende semiconductor by single color pulses

M. Bieler,^{a)} N. Laman, and H. M. van Driel^{b)}

Department of Physics, University of Toronto, Toronto, Ontario M5S1A7, Canada

Arthur L. Smirl

Laboratory for Photonics and Quantum Electronics, 138 IATL, University of Iowa, Iowa City, Iowa 52242

(Received 13 October 2004; accepted 10 December 2004; published online 1 February 2005)

Ultrafast ballistic electrical currents are generated through interband excitation of strained InGaAs/GaAs quantum well samples at 295 K by 810 nm, 60 fs circularly polarized optical pulses. These currents are generated through quantum interference of optical absorption pathways associated with the orthogonally polarized components of the light field, and although the spin of the currents is not directly measured, they should also be spin polarized. The femtosecond transient currents are detected via the emitted terahertz (THz) radiation which has a bandwidth of ~ 8 THz. The THz amplitude scales linearly with injected carrier density up to $\sim 10^{18}$ cm⁻³ beyond which state filling and carrier-carrier scattering cause a sublinear dependence. A peak current density of 9 kA/cm² is obtained for a peak pump intensity of 250 MW/cm². © 2005 American Institute of Physics. [DOI: 10.1063/1.1855426]

The application of the electron's spin degree of freedom in technology has spawned the field of spintronics.¹ A necessary requirement for many future active devices is the ability to generate and control spin-polarized electrical currents or pure spin currents. Such currents can be generated purely electrically in semiconductors by, e.g., injection from ferromagnetic metals. However optical techniques offer an alternative and noninvasive way to generate spin currents without the need of magnetic materials. One way to optically induce electrical or spin currents in high-symmetry semiconductors such as GaAs is through the quantum interference and control (QUIC) of single and two-photon absorption pathways.^{2,3} In lower symmetry semiconductors, QUIC can be used with a single color beam to inject a spin-polarized electrical current through interference of absorption pathways associated with orthogonally polarized beam components.⁴ This effect can also be understood as a second-order nonlinear optical process;⁵ since the maximum effect occurs for circularly polarized light, it is also referred to as the circular photogalvanic effect.⁶ Single beam induced QUIC currents have been observed following *interband* excitation of wurtzite CdSe⁴ or *p*-type GaAs/AlGaAs quantum wells (QWs)⁶ and by *intraband* excitation of QWs.^{7,8} For the experiments reported by Bel'kov *et al.* the low crystal symmetry came from a (113)A-cut QW material (C_3 symmetry). In all these cases no time resolution was attempted; the currents were detected via charge accumulation at electrodes. In this letter we use strain to lower the symmetry of a (110) oriented zinc blende semiconductor and efficiently induce large QUIC currents. Using 60 fs, 810 nm excitation pulses we generate femtosecond time-scale ballistic currents that are detected by their emitted terahertz (THz) radiation. The injected current scales linearly with carrier density up to 10^{18} cm⁻³, above which a sublinear behavior is observed and

attributed to state filling and the increasing role of carrier-carrier scattering.

The dynamics of QUIC currents generated by a single beam can be expressed through⁴

$$\frac{dJ^a}{dt} = \eta_{abc} E_b E_c \sin(\phi_b - \phi_c) - \frac{J^a}{\tau_s}. \quad (1)$$

Here, $E_{b,c}$ are orthogonal components of the beam with phase $\phi_{b,c}$, η_{abc} is a third rank tensor which is antisymmetric with respect to exchange of the last two indices, and τ_s is the momentum scattering time. The largest current is induced for $\phi_b - \phi_c = \pm \pi/2$, i.e., circularly polarized light; the current vanishes for linearly polarized beams ($\phi_b - \phi_c = 0, \pi$). In bulk zinc blende materials with a point group T_d , the tensor η vanishes; however, it has nonzero elements in materials with lower point group symmetry.^{4,5}

Our sample consists of 20 undoped GaAs/In_{0.13}Ga_{0.87}As QWs that are grown in the [110] direction. The barriers and wells are both 8 nm wide, and the QW region is embedded in an Al_{0.3}Ga_{0.7}As PIN structure. As will be seen in the following, the PIN structure does not influence the QUIC process. In principle, the same experiments can be performed without the QWs being embedded in such a structure. Of primary importance is the indium concentration in the wells which leads to a lattice mismatch of $\sim 1\%$ between the GaAs barriers and InGaAs wells. A uniform strain of 1% in the plane of the QWs leads to $\sim 1\%$ uniaxial strain along the growth direction⁹ reducing the point group symmetry to C_{2v} .¹⁰ For such a sample the tensor element η_{xyx} is nonzero. As shown in Fig. 1, x and y are taken along the [001] and $[1\bar{1}0]$ directions with z being along the [110] direction, the surface normal direction and the direction of light propagation.

The experimental setup is shown in Fig. 1. An 80 MHz Ti:sapphire oscillator produces 60 fs, 810 nm pulses which are directed at normal incidence onto the sample with a focused spot size of 80 μ m (full width at half maximum). THz radiation emitted by the transient current induced near the sample's front surface is collected by an off-axis parabolic

^{a)}Present and permanent address: Physikalisch-Technische Bundesanstalt, Bundesallee 100, D-38116 Braunschweig, Germany.

^{b)}Electronic mail: vandriel@physics.utoronto.ca

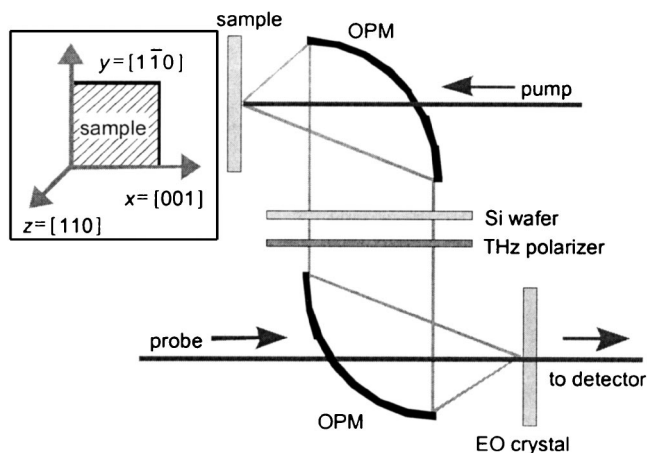


FIG. 1. Experimental setup. OPM: off-axis parabolic mirror. The inset shows the sample; pump light is incident along the z direction.

mirror and directed to a second off-axis parabolic mirror. The second mirror focuses the THz radiation onto an electro-optic (EO) crystal, which is either a 500- μm -thick, (110)-oriented ZnTe crystal or a 120- μm -thick, (111)-oriented GaP crystal. The GaP crystal provides higher bandwidth whereas the ZnTe crystal is more sensitive to the THz fields. An 810 nm, 60 fs probe pulse is focused on the EO crystal to a spot size of 350 μm , overlapping the THz focal spot. The pump and probe beams are focused onto the sample and the EO crystal, respectively, through small holes in the off-axis parabolic mirrors. A silicon wafer placed between the two parabolic mirrors blocks any reflected and scattered pump light. A THz polarizer is also used to block any THz radiation that arises from currents along the sample's [001] direction (see inset of Fig. 1). Two different contributions to the current might arise along this direction, namely, (i) a shift current¹¹ and (ii) a current due to the piezoelectric effect whereby strain along the [110] direction leads to a field and current along the [001] direction.

For right- and left-handed circularly polarized pump pulses, Fig. 2(a) shows the time-dependent THz signal from currents traveling in the $[1\bar{1}0]$ direction and detected using the GaP crystal. The π phase change of the THz signal when the pump helicity is reversed is consistent with current injection via the single color QUIC effect as indicated by Eq. (1). As expected no measurable signal is obtained for linearly polarized pump light. From the well-known selection rules for carrier excitation by circularly polarized light the injected currents are expected to be spin polarized.

In the absence of carrier momentum scattering, the injection current would be proportional to the integral of the optical pulse. With scattering the current decays in accordance with Eq. (1). To examine aspects of the decay kinetics we have measured the THz signatures associated with different pump intensities. Figure 2(b) shows the normalized power spectra of these currents for peak pump intensities of 250 MW/cm^2 , 800 MW/cm^2 , and 1.2 GW/cm^2 , corresponding to carrier densities of 1.1, 3.4, and 5.1 $\times 10^{18} \text{ cm}^{-3}$, respectively. All three spectra peak at ~ 2 THz and overlap to within experimental error, indicating that the actual temporal shape of the THz emission does not change significantly up to a carrier density of 5.1 $\times 10^{18} \text{ cm}^{-3}$. The time resolution of our experiment is mainly limited by the

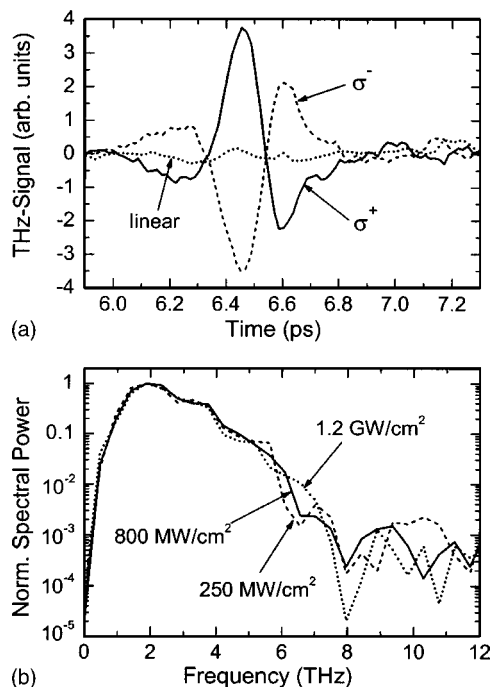


FIG. 2. (a) THz signals from injected currents directed along the $[1\bar{1}0]$ direction for right-handed (solid line, σ^+) and left-handed (dashed line, σ^-) circularly polarized light. Dotted line: recorded signal for linearly polarized light. (b) Normalized power spectra of the THz pulses for σ^+ pump polarization at three different intensities: 250 MW/cm^2 (dotted line), 800 MW/cm^2 (solid line), and 1.2 GW/cm^2 (dashed line).

mismatch of the probe group velocity and the THz pulse phase velocity in the GaP crystal and as can be seen from Fig. 2(b) the measured power spectra have a 30 dB point at ~ 8 THz. Taking into account the 60 fs optical pulse width and the signal-to-noise ratio numerical simulations show that the momentum scattering time of the carriers is less than 50 fs, consistent with previous measurements in bulk GaAs.¹²

We have also examined the density dependence of the QUIC current amplitude over a wide pump intensity range using the more sensitive ZnTe crystal, which is more appropriate here since the shape of the THz pulse is not essential. Figure 3 shows the THz signal amplitude versus pump intensity. A sublinear behavior occurs near a peak intensity of 400 MW/cm^2 , corresponding to a carrier density of 1.6 $\times 10^{18} \text{ cm}^{-3}$. A sublinear dependence was also observed for injection currents generated by quantum interference of one- and two-photon excitation¹³ and attributed to a combination of state filling, space-charge field effects, and the onset of

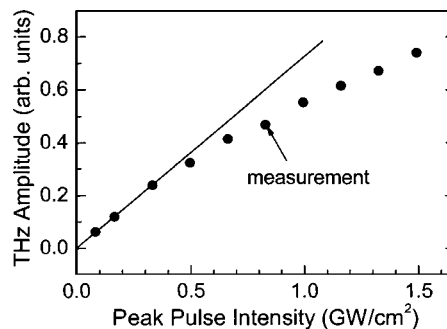


FIG. 3. Amplitude of THz pulses as a function of pump intensity. Closed circles: experimental data, black line: linear fit to the first four data points, including origin.

carrier–carrier scattering. For the case here, a hydrodynamic model calculation shows that field effects are small and so the sublinear density behavior is attributed to state filling and the onset of carrier–carrier scattering.

The peak QUIC current density can be estimated from the peak electric THz field extracted from the measured EO signal¹⁴ by using the THz propagation code described in Ref. 15. For a peak pump intensity of 250 MW/cm² we obtain values of 0.25 V/cm and 9 kA/cm² for the peak THz field and the peak current density, respectively.

Finally we comment further on the role of the QWs and the *PIN* structure. Even unstrained QWs introduced into the (110)-oriented materials reduce the point group symmetry to C_{2v} and the built-in electric field from a *PIN* structure leads to a further reduction to C_s . To exclude the quantum wells or the built-in electric field in our sample as the origin of the QUIC current, we attempted to measure an injection current in an unstrained (110)-grown GaAs/Al_{0.3}Ga_{0.7}As QW sample that was otherwise identical to the InGaAs/GaAs sample (including the AlGaAs *PIN* structure). No measurable QUIC current was observed. Based on the signal-to-noise ratio in our experiments we conclude that the QUIC effect in the unstrained GaAs/AlGaAs sample is at least 20 times smaller than that in the strained material.

In summary, we have generated spin-polarized ballistic currents in strained zinc blende QWs following optical interband excitation with 60 fs optical pulses and observed the ultrafast currents through their emitted THz radiation. The strain that is incorporated in the InGaAs/GaAs QWs, a material routinely used for telecommunication devices, provides a QUIC current which is not observed in unstrained materials. For a peak pump intensity of 250 MW/cm² at 810 nm a peak current of 9 kA/cm² is obtained in the strained InGaAs/GaAs material. At carrier densities above 10¹⁸ cm⁻³ the THz amplitude has a sublinear dependence on the pump

intensity, which we attribute to state filling and the carrier dependence of the momentum scattering time.

The authors thank J. E. Sipe and members of his research group for valuable and enlightening discussions. In addition we appreciate financial support from the Sciences and Engineering Research Council of Canada, Photonics Research Ontario, and DARPA.

¹D. D. Awschalom, D. Loss, and N. Samarth, *Semiconductor Spintronics and Quantum Computation* (Nanoscience and Technology Series), edited by K. von Klitzing, H. Sakaki, and R. Wiesendanger (Springer, Berlin, 2002).

²A. Haché, Y. Kostoulas, R. Atanasov, J. L. Hughes, J. E. Sipe, and H. M. van Driel, *Phys. Rev. Lett.* **78**, 306 (1997).

³M. J. Stevens, A. L. Smirl, R. D. R. Bhat, A. Najmaie, J. E. Sipe, and H. M. van Driel, *Phys. Rev. Lett.* **90**, 136603 (2003).

⁴N. Laman, A. I. Shkrebtii, J. E. Sipe, and H. M. van Driel, *Appl. Phys. Lett.* **75**, 2581 (1999).

⁵J. E. Sipe and A. I. Shkrebtii, *Phys. Rev. B* **61**, 5337 (2000).

⁶V. V. Bel'kov, S. D. Ganichev, P. Schneider, C. Back, M. Oestreich, J. Rudolph, D. Hägele, L. E. Golub, W. Wegschneider, and W. Prettl, *Solid State Commun.* **128**, 283 (2003).

⁷S. D. Ganichev, E. L. Ivchenko, S. N. Danilov, J. Eroms, W. Wegschneider, D. Weiss, and W. Prettl, *Phys. Rev. Lett.* **86**, 4358 (2001).

⁸S. D. Ganichev and W. Prettl, *J. Phys.: Condens. Matter* **15**, R935 (2003).

⁹S. L. Chuang, *Physics of Optoelectronic Devices* (Wiley, New York, 1995).

¹⁰G. L. Bir and G. E. Pikus, *Symmetry and Strain-induced Effects in Semiconductors* (Wiley, New York, 1974).

¹¹D. Côté, N. Laman, and H. M. van Driel, *Appl. Phys. Lett.* **80**, 905 (2002).

¹²M. T. Portella, J. Y. Bigot, R. W. Schoenlein, J. E. Cunningham, and C. V. Shank, *Appl. Phys. Lett.* **60**, 2123 (1992).

¹³D. Côté, J. M. Fraser, M. DeCamp, P. H. Bucksbaum, and H. M. van Driel, *Appl. Phys. Lett.* **75**, 3959 (1999).

¹⁴P. C. M. Planken, H.-K. Nienhuys, H. J. Bakker, and T. Wenckebach, *J. Opt. Soc. Am. B* **18**, 313 (2001).

¹⁵D. Côté, J. E. Sipe, and H. M. van Driel, *J. Opt. Soc. Am. B* **20**, 1374 (2003).